# Simulation of two-step redox recycling of non-stoichiometric ceria with thermochemical dissociation of $CO_2/H_2O$ in moving bed reactors --Part II: Techno-economic analysis and integration with 100 MW oxyfuel power plant with carbon capture

**Abstract:**

This paper presents a solar thermochemical looping $CO_2/H_2O$ dissociation reactors unit (CL) with commercial ceria as redox oxygen carrier. The CL unit is integrated to a 100 MW oxy-fueled natural gas combined cycle with carbon capture to investigate the efficiency benefit obtained. A moving bed counter-current reactor model is developed in Aspen Plus considring rigorous continuous stirred reactors (RCSTRs) for both reduction and oxidation. A user-kinetic subroutine is developed in FORTRAN and linked with each RCSTR in both reduction and oxidation reactor with their respective kinetics. It is found that efficiency of the chemical looping unit varies widely with reduction reactor temperature and vacuum pressure. Chemical looping unit efficiency is obtained for three conditions considering only $CO_2$ and only $H_2O$ it was found to be 35.41% and 30.84% respectively, and for mixture (86% $CO_2$, 14% $H_2O$) 35.26%. The efficiency drop for only $H_2O$ is due to heat needed for phase change and more vacuum pump required for hydrogen compare to $CO_2$. The maximum solar to electrical efficiency for the whole system layout was found to be 25.4% with a reduction temperature of 1600$^oC$ and $10^{-7}$ bar vacuum pressure. With a 0.5 $m^3$ reduction reactor and 5 $m^3$ oxidation reactor the maximum net electricity produced by add-on unit is 12.85 MWe. Economic analysis revealed that the major contributor to the total project cost is hydrogen compressor (19%) and solar field and tower represent 39% of the total equipment costs giving a specific overnight capital cost of 12136 $/kW with LCOE of 1100 S/MWh.

**Keywords:** Solar fuels, Reaction kinetics, Techno-economic, Carbon capture and sequestration, Chemical looping.

# 1 Introduction:

Ever increasing energy demand and still huge amount of fossil reserves force us to use fossils which will lead to increase in emissions. If measures are not taken to curb the increasing

emissions especially $CO_2$ then the target set to limit the temperature rise of 2$^oC$ will not be met [1]. Therefore, the need for searching alternatives to meet energy requirement is on peak. Sustainable sources such as solar energy which is readily available to harness and many methods have been explored to exploit and produce power or chemicals ) [2–4]. Solar thermochemical cycles have been extensively studied in the past couple of years as a promising step to curb the carbon dioxide emissions and to convert them into synthetic fuels or chemicals for industrial application [5]. The process involves two steps with first step involving solar thermal reduction of metal oxides (also called as oxygen carrier) to lower valence state releasing oxygen (endothermic step) and second step, where the metal oxide gets oxidizes converting $CO_2$/$H_2O$ into CO/$H_2$ (exothermic step) with metal oxides undergoes continuous reversible redox reactions. Usually solar thermal reduction occurs above 1300$^oC$ and under vacuum conditions and oxidation reaction above 800$^oC$ and at near atmospheric pressure condition [6]. In any chemical looping process, the oxygen carrier (OC) plays an important role and following characteristics is sought in selection. OCs should be mechanically stable and should be agglomeration and attrition resistant, redox recyclable to maintain similar oxygen carrying capacity in each cycle [7]. In the past decade the many OCs have been investigated from volatile (ZnO, $SnO_2$) to non-volatile-stoichiometric ($Fe_3O_4$, Ferrites, Hercynite) and non-volatile-non-stoichiometric (such as $CeO_2$, doped ceria and perovskites) [8].

Among all the reported OCs, ceria is the most investigated due to its faster redox kinetics, recyclability and good electrochemical properties [9]. In order to reduce the reduction temperature ceria is doped with tetravalent and trivalent cations that increases the oxygen carrying capacity during redox reaction [10]. Since these materials are still in development stage and availability in terms of large scale is major issue, therefore ceria is selected for the present investigation. Equation (1-3) represents thermal reduction and oxidation reaction and the schematic of the solar thermochemical looping is shown in Fig 1.

$$\text{Reduction reactor}: CeO_2 \xrightarrow[T_1]{\Delta H_1} CeO_{2-\delta} + 0.5\delta O_2 \quad (1)$$

$$\text{Oxidation reactor}: CeO_{2-\delta} + \delta CO_2 \xrightarrow[T_2]{-\Delta H_2} CeO_2 + \delta CO \quad (2)$$

$$\text{Oxidation reactor}: CeO_{2-\delta} + \delta H_2O \xrightarrow[T_2]{-\Delta H_2} CeO_2 + \delta H_2 \quad (3)$$

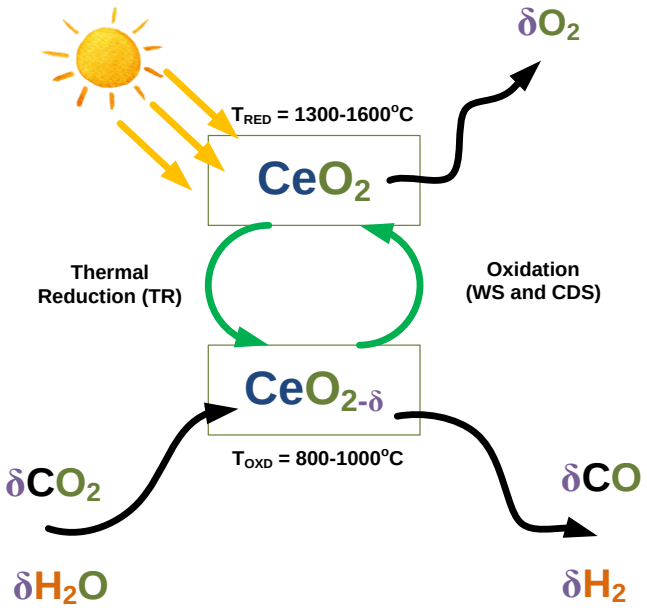


*Figure 1 Schematic of solar thermochemical $CO_2/H_2O$ dissociation for $CO/H_2$ production*

In literature many solar reactors have been proposed and classified among as structured and non-structured. The configurations include fixed bed (packed bed), parallel flow and counter-current flow [11] but analysis reported is based on thermodynamics and Gibbs minimization principle. Bulfin et al [12] reported the thermal reduction kinetics for non-stoichiometric ceria based on forward and backward reaction principle. The model presented is validated against experimental results and are presented in parallel paper [paper 1 reference]. Oxidation kinetics of $CO_2$ and $H_2O$ splitting is presented by Arifin [13] was utilized for the model development. Multiple RCSTRs in series is connected for both reduction and oxidation with user-kinetic subroutine hooked to each RCSTR. The CL model is then connected to oxy-fuel power plant with 100% carbon capture. Presently oxy-fuel combustion technology has received huge interest among fossil based carbon capture power plant [14,15]. In oxy-fuel power plant, oxygen is supplied in combustion chamber instead of air which increases the efficiency and making carbon capture as the exhaust does not have NOx emissions. Air separation unit (ASU) is used for separation of oxygen from air to feed the combustion chamber and the exhaust of combustion chamber would be only $CO_2$ and $H_2O$ and water

would be separated by condenser leaving pure $CO_2$. Usually oxy-fuel combustion is utilized for retrofitting natural gas combined cycle (NGCC) but it requires change in designing the turbines and compressors providing the high efficiency of carbon capture (~99%)[16].

Kong et al [17] investigated a polygeneration system that operates isothermal redox reaction of ceria at 1600$^{o}$C with reduction reactor operating at $10^{-5}$ bar and oxidation reactor at 1 bar considering Gibbs minimization. The downstream process from oxidation reactor undergoes a reforming leading to power and methanol production. Solar to syngas efficiencies ($\eta_{SCL}$) in chemical looping unit operating at mention operating conditions gives 45.7% with only $CO_2$ splitting and 38.1% for water splitting. Kong et al [18] also studied a comparison of temperature swing and isothermal redox cycle considering at 1650$^{o}$C and $10^{-5}$ bar. The argument presented raised the issue of heat recovery system between a two-temperature swing redox cycle and concluded that it's a trade-off between thermal and material consideration and concluded the efficiency obtained for $CO_2$ splitting is 28%. Most of the studies presented considers the thermodynamics for redox reaction but due to the nature of the non-catalytic heterogeneous reactions it is important to consider the reaction kinetics as it plays major role in reaction time that determines the residence time and recirculation between reduction and oxidation that defines the reaction extent in each cycle. Chemical looping for thermo-chemical dissociation of the captured $CO_2$, by producing fuel from $H_2O$/recycled $CO_2$, has exciting potential to improve the system efficiency by providing additional fuel.

In this regard, considering chemical looping syngas production still a developing technology, the reactor design and operation feasibility were considered to utilized while retrofitted to a scale of 100 MW Power Plant with CCS. A simple Oxyfuel NGCC with CCS was modelled to evaluate the net $CO_2$ and water generated.

The end use of the $CO/H_2$ produced varies based on local needs, plant design and configuration ranging from power production to the production of chemicals like methane or fuels or advanced Fischer Tropsch liquids. However, for such polygeneration systems, no direct definition of efficiency exists [19]. Hence to evaluate the primary benefits of the excess fuel generation by chemical looping splitting, a solar thermochemical cycle dedicated to power generation from the excess fuel produced was conceived. A conceptual layout development, with a performance assessment, has been subsequently studied as a technology feasibility assessment of such integrations and possibilities of scaling up to utility scales.

# 2 Plant Layout and Configuration

The most efficient conventional fossil fuel power plant is considered to be natural gas combined cycle (NGCC) with its efficiency reaching to 57% based on it lower heating value.[20]. Integrating a carbon capture and sequestration(CCS) to the conventional NGCC plants decreases the $CO_2$ emission to a level less than 100g $CO_2$/kWh from different technologies reported in the literature [20–22]. Of all the CCS technologies oxyfuel combustion has minimum modification the plant layout and having capability of capturing 100% $CO_2$, but this leads to decrease energy penalty decreasing the efficiency to large extent. Hence, an add-on unit, utilizing the thermal reduction of ceria by a concentrated solar power with the corresponding splitting of a part of the gaseous exhausts ($CO_2$ and/or $H_2O$) has been proposed for syngas (fuel) and subsequently power generation to improve on the suffered energy penalty from carbon capture. A part of the stream of pure $CO_2$ and wastewater generated in the CCS unit has been proposed to be utilized within the add-on unit. Figure 2 below shows the plant layouts and configuration of the proposed solar thermochemical power system to be set as an add-on unit to an oxyfuel power unit with CCS. It needs to be clarified that the add-on unit is not limited to integration with only NGCC. The availability of pure

$CO_2$ and $H_2O$ from other oxyfuel power plants with different feedstock (coal and oil) would allow the proposed add-on unit to be integrated different oxyfuel power plants.

The add-on plant primarily comprises the chemical looping (CL) unit consisting of reduction and oxidation reactor, for the generation of syngas from the splitting of recycled $CO_2$ and /or $H_2O$. The reduction reactor would be operated under vacuum as solar thermal reduction is favour at very low partial pressure of oxygen. Several heat exchangers need to be employed for heat integration within the system for $CO_2$ heating or steam generation for splitting, as well as steam generation from the excess heat for expansion in the steam turbine. Indeed, all the excess heat in the present layout has been integrated to heat recovery steam generation (HRSG) for subsequent steam generation and use in a single bottoming steam cycle. Irrespective of the gas composition an oxyfuel combustion configuration of the produced syngas has been considered. The exhaust gases would then be and sent back for CCS, either by employing a separate clean-up unit or through minor modifications to the existing condenser of the CCS unit. Since the reduction reactor is operated under vacuum conditions, pure oxygen is produced, which has been proposed to be utilized in the combustor for power generation. This would decrease the need for oxygen from an additional air separation unit. The oxidation reactor would be operated at 2 bar pressures instead of at atmospheric conditions to decrease the compression work of the produced CO and/or $H_2$ needed for the corresponding operation of the combined cycle.

The solar field can either be a central tower configuration, or a beam down configuration. Indeed, the reactor design concept presented by Muhich et al [23] utilizes a beam-up reactor concept via a central tower, where the oxidation reactor is a fluidized bed reactor. With regards to the understanding of operability of the fluidized bed reactor a huge volume of the gas is required to fluidization would certainly decrease the selectivity of the CO and $H_2$

produced to very low value which limits the application of fluidized bed reactor for oxidation. Therefore, in the present layout a moving bed reactor has been considered for the oxidation (as reported in paper I), the beam down reactor configuration might seem to be easier to operate, especially with regards to solids handling between the reduction and the oxidation reactor. Nevertheless, solar field design considerations have not been included in the present study, except for the necessary performance evaluation of the proposed add-on unit, though the assumption of solar field efficiency.

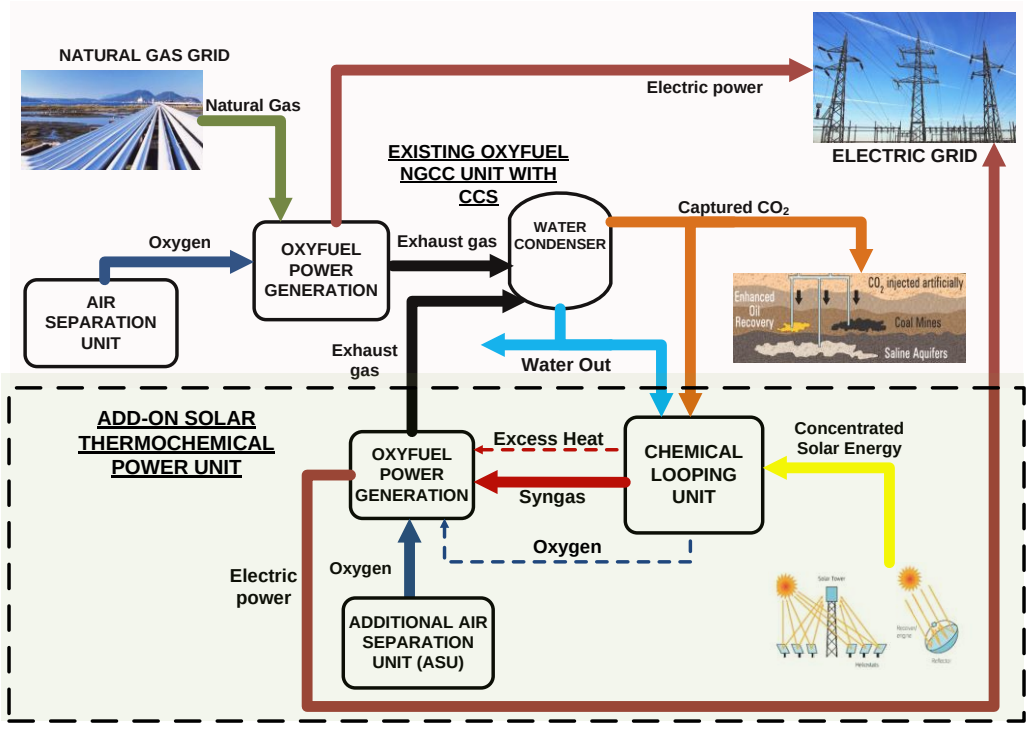


*Figure 2 Solar Thermochemical plant Conceptual layout with $CO_2$ and/ or $H_2O$ recycling for power generation*

## 2.1 System modelling in ASPEN Plus

The detailed plant schematics of the Solar Chemical Looping Power Generation add-on unit with oxyfuel combustion involving $CO_2$ and/or $H_2O$ dissociation and carbon capture (SCLP-OXY-CC) has been presented and discussed. Subsequent evaluation of the proposed add-on

unit was carried out in ASPEN Plus® (v 8.8) and its corresponding existing functions and built-in modules. The PR-BM method was selected for the simulations.

### 2.1.1 Assumptions

The generic assumptions used in the present simulation are listed below:

- Steady-state simulations were performed, and the results hence obtained are not applicable to start-up or transient operations.
- Reduction (RED) and oxidation reactor (OXI) is modelled as moving bed reactors as presented in our parallel work [paper part 1 reference].
- The maximum Turbine Inlet Temperature (TIT) of 1377ºC was considered, within the range of maximum TIT of commercially available gas turbines [24].
- The maximum pressure ratio for a single stage expansion in a stationary gas turbine is 18:1 as of commercial gas turbines [25]. This limit was respected within the present layout as well.
- No heat loss and inefficiencies are considered within in the lines.
- The ambient condition was assumed as 25ºC and 1.013 bar. Also, the composition of air was assumed to comprise 79% $N_2$ and 21% $O_2$ on a volume basis.
- Minimum approach temperature in heat exchangers was taken as $10^{o}$C [26].
- The isentropic efficiency and mechanical efficiency for compressors and turbines were considered as 0.9 and 0.98, respectively. The pump efficiency was assumed to be 0.85 and 0.9, for isentropic and mechanical efficiency respectively.
- The primary objective of the present study is to recognize the potential efficiency gain from the addition of the chemical looping and a downstream power generation unit in a conventional oxyfuel plant. Hence the turbines and the HSRG were modelled as simple units, without reheating or multi-pressure systems. Indeed, by increasing the

model complexity, together by performing design optimization, the net efficiency can be improved considerably by process optimization studies.

Moreover, design assumptions with respect to individual units of the respective layouts are listed in the table 1.

A simplistic model of a 100MW power NGCC and a corresponding oxyfuel NGCC power plant of the same capacity with CCS was developed in ASPEN Plus, incorporating all the necessary assumptions stated above. This was necessary to evaluate the performance of the base case power plants, together with the availability of $CO_2$ and $H_2O$ necessary for added fuel generation via splitting. Since the primary aim of the present study is to develop the feasibility investigation of integration of the splitting cycle in an add-on unit and to evaluate the net benefit from the generation of additional electricity, the need for detailed modelling of the base case was not considered crucial. The net molar flow of $CO_2$ to the carbon capture and sequestration unit from the base case of 100 MW oxyfuel NGCC with CCS was obtained around 330 mol/s. The corresponding water released from the condenser of the exhaust gas was 550 mol/s. For the layouts of the base case power plants with and without CCS integration without CL unit as modelled in ASPEN Plus and can be seen in Farooqui et al [27].

From the limitation of the present technology development of not only the CL unit but also on the perspectives of concentrated solar technology and the possibility of providing high-temperature heat over a large control volume, the use of 20% of $CO_2$ from the CCS unit was considered for splitting in the base case scenario. The molar flow of gas for splitting would thus be 66 mol/s. Corresponding water utilization for the base case scenario is 12%. The ceria flow was calculated accordingly and has been discussed in subsequent sections.

## 2.2 Simulation Description

A common configuration of the add-on, applicable irrespective of the gas mixture into the oxidation reactor was then modelled and simulated in ASPEN Plus. Figure 3 shows the system configuration developed.

*Table 1* Design assumptions used for developing the process flowsheet models in ASPEN plus

| Unit | Parameters |
|---|---|
| ASU | • $O_2$ purity: 99.9% (by volume)<br>ASU $O_2$ and $N_2$ delivery pressure: 1.2 bars<br>$O_2$ compression pressure: 18 bars<br>A small fraction of the $N_2$ was used as sweep gas in CL unit |
| Solar Field | • A generic solar field efficiency of 75% was assumed based in the consideration of a central receiver configuration [28].<br>• Thermal Receiver efficiency was assumed as 89% [29]. |
| Reduction Reactor (RED) and Thermal Receiver | • An isothermal reactor at 1600$^{o}$C and a vacuum pressure of $10^{-7}$ bar was considered for the base case scenario.<br>• Continuous metal oxide transportation between the oxidation reactor (OXI) and reduction reactor (RED) reactors was assumed, neglecting work expended in metal oxide handling. |
| Oxidation reactor (OXI) | • An adiabatic reactor with adequate insulation to ensure no heat loss was considered.<br>• The oxygen carrier outlet temperature from OXI was considered as the oxygen carrier inlet temperature to RED |
| Vacuum Pump (VACPMP) | • Modelled as a four-stage compressor with inter-cooling<br>• Isentropic efficiency: 90%<br>• Mechanical efficiency: 98%<br>• Discharge pressure: 1 atm |
| Compressors | • Isentropic efficiency: 90%<br>• Mechanical efficiency: 98% |
| Combustor (COMB) | • Excess oxygen factor of 1.05 for CO and/or CO and $H_2$ mixture combustion considered.<br>• Pressure drop within combustor: 0.2 bar<br>• Heat loss from combustor: 0.2 MW |
| Gas Turbine | • Isentropic efficiency: 90%<br>• Mechanical efficiency: 98% |
| Steam Turbine and HRSG | • Single stage expansion in the steam turbine was considered.<br>• Turbine isentropic efficiency: 90%<br>• Mechanical efficiency: 98%<br>• Steam Pressure: 150 bars<br>• Live steam temperature for steam turbine inlet: 600$^{o}$C<br>• Condenser pressure: 0.04 bar<br>• Pump isentropic efficiency: 0.8 |

The heart of the proposed SCLP-OXY-CC add-on unit is the chemical looping (CL) unit, modelled as moving bed reactors, as per the reactor model developed in ASPEN Plus and discussed in the previous section. For the reduction reactor (RED), a vacuum pump (VACPMP) is necessary to maintain the vacuum pressure and has been modelled as a four-stage compressor with inter-cooling. The oxygen from the RED (Stream 14) is first cooled and then released at atmospheric pressure by the vacuum pump. The heated and reduced metal oxide from the RED (Stream 25) is then cooled in steps, modelled as two heat exchangers (METHX-1 and METHX-2) for simplicity. The first heat exchanger would conceptually be used to heat up the inlet gas mixture to the oxidation reactor (OXI) in the form of steam generation in STEAMGEN or $CO_2$ heating. METHX-2 would then ensure the necessary metal oxide inlet temperature to the OXI via steam generation. This would, however, limit the plant operation at lower temperatures of the reduction reactor due to the chances of temperature cross-over for a constant feed temperature to the OXI.

The product gas from the OXI (Stream 6) is first cooled against steam generation till ambient temperature and subsequently passed through a condenser to remove the moisture (COND-1). However, this becomes a redundant unit while working with only $CO_2$, wherein no water is present in the product gas. Subsequently, the syngas (Stream 19) is compressed in SYNCOMP to a pressure of 18.2 bar and fed into the combustor. Since the exhaust gas needs to be fed back to the CCS stream, an oxyfuel combustion is necessary. Excess $O_2$, as required for the combustion (Stream 18) is sourced from an additional air separation unit and compressed together with the oxygen from the RED for the combustor. Since near stoichiometric oxygen necessary for the combustion of syngas is produced from the reduction reactor, the size of the ASU required is significantly small in comparison to the scale of the

add-on unit. Thus, a significant energetic benefit from the internal use of the generated oxygen can be obtained, countering the energy penalty of vacuum generation for reduction.

In the combustion chamber (COMB), a pressure drop of 0.2 bar results in the inlet pressure to the gas turbine (GT) of 18 bars. The temperature at the combustor outlet, or in other words, the turbine inlet temperature (TIT) is maintained at 1377$^{o}$C by recycling $CO_2$ from the CCS stream (Stream 29) via a $CO_2$ compressor (CO2COMP). The exhaust gas from the combustion chamber (COMB) is expanded in a gas turbine (GT) up to a pressure of about 1.04 bar and further subsequently fed to an HRSG for steam generation to be used in the bottoming steam cycle. Due to the absence of $SO_x$, the gas can be expanded to temperatures as low as 50$^{o}$C. The exhaust gas, after water condensation, comprises almost pure $CO_2$ (Stream 13). Therefore, it would be sent back to the CCS stream from where it was originally sourced from. Thus, the zero-emission system of the original plant is maintained, as can be visualized in the plant layout detailed in the Figure 3.

A major advantage of the proposed cycle working with or without $CO_2$ is the fact that the entire cycle continues at the same molar flow of the sourced $CO_2$ from the CCS stream, with no additional product being generated to that of the recycled $CO_2$. This simplifies the integration of the add-on unit to the original power plant significantly, by requiring minimum additions or changes for the necessary retrofit. Indeed, a direct utilization of the exhaust of the original Oxyfuel power plant, which essentially is a mixture of approximately 86% of $CO_2$ and about 14% of $H_2O$ would be of significant interest. Hence, analyses with three possible gas mixtures, only $CO_2$, only $H_2O$ and a $CO_2/H_2O$ mixture replicating the typical exhaust of an oxyfuel power plant were performed to evaluate the performance of the SCLP-OXY-CC add-on unit with respect to the gas composition to the OXI.

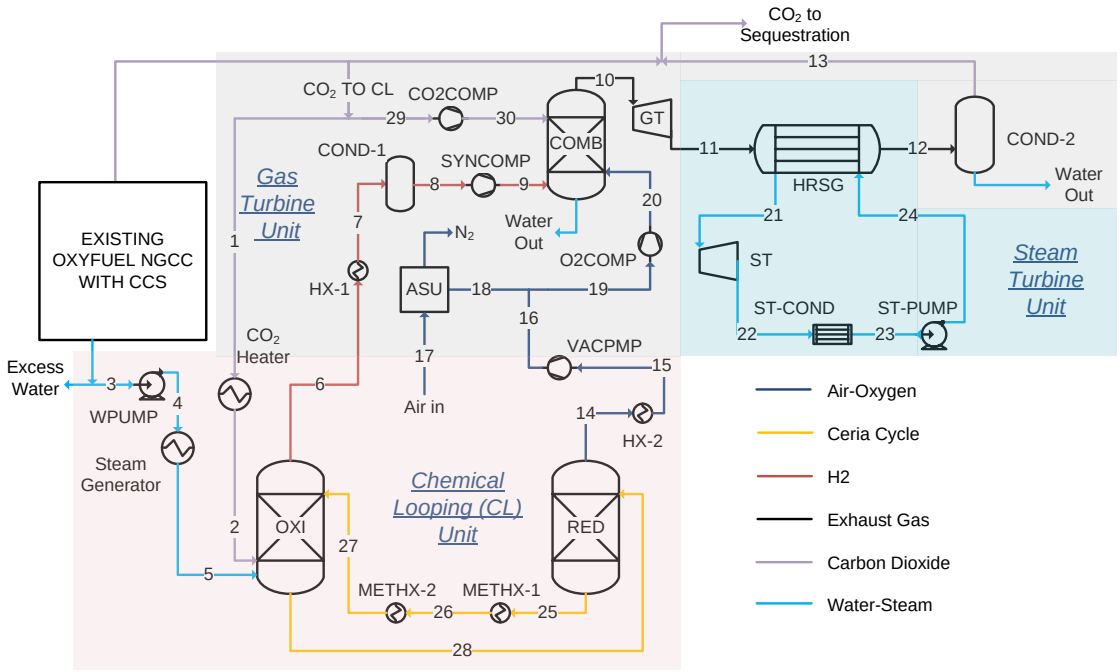


*Figure 3 Conceptual layout of the SCLP-OXY-CC add-on unit utilizing $CO_2$ and/or $H_2O$ splitting with thermal reduction of ceria recycling for power generation via fuel-air combustion*

## 2.3 Energy Performance Evaluation

To obtain the comparative thermodynamic system performance of the add-on solar thermochemical power plant with respect to individual efficiency and with respect to the combined efficiency with the oxyfuel power plant, an energy analysis is necessary to be evaluated.

The energy analysis is based on the first law of thermodynamics and considers the principle of conservation of energy applied to a prescribed system. The thermal efficiency of the proposed power plant, directly concluded based on the first law of thermodynamics is therefore evaluated in terms of the rate at which solar power ($\dot{Q}_{sol}$) is converted to the net electric power output ($\dot{W}_{el,net}$) [30], as defined by the following equation (4):

$$\eta_{th} = \frac{\dot{W}_{el,net}}{\dot{Q}_F} = 1 - \frac{\dot{Q}_L}{\dot{Q}_F} \qquad (4)$$

Where, $\dot{Q}_L$ is the system energy loss. However, for components such as pumps or compressors, where the thermal efficiency is not possible to be evaluated in terms of useful energy output, the thermodynamic performance is assessed via the concept of 'isentropic efficiency'. By this, a comparative analysis is developed between the actual and ideal performance of a device. The ideal conditions are related to no entropy generation, together with negligible heat transfer between the device and the surrounding [31]. Nevertheless, beyond the thermal efficiency of the power plant, the efficiency of the receiver and the solar field play a crucial role in the overall solar to electricity of the proposed add-on unit. Indeed, this limits the overall performance of the proposed SCLP-OXY-CC unit. For a solar field efficiency of $\eta_{sol\text{-}field}$, and a receiver efficiency denoted by $\eta_{reciever}$, the solar to electricity efficiency of the proposed add-on unit ($\eta_{sol\text{-}e}$) can be written as per the following equation (5). In the following analysis, the solar-to-electricity efficiency has usually been referred to describe the SCLP-OXY-CC plant efficiency, unless otherwise mentioned.

$$\eta_{sol-e} = \eta_{th} \times \eta_{sol-field} \times \eta_{receiver} \tag{5}$$

However, in addition to the net plant efficiency of the add-on unit, interest lies in the study of the CL unit efficiency in itself. The efficiency is derived based on the similar principle described above, however, the output being the net chemical potential in the split gas in terms of its lower calorific value (LHV). The definition of efficiency for the CL unit has been defined as follows by equation (6).

$$\eta_{SCL} = \frac{(\dot{m}_{H_2} LHV_{H_2} + \dot{m}_{CO} LHV_{CO})_{oxy}}{(\dot{Q}_{red} - \dot{Q}_{oxd}) + \dot{Q}_{CO_2/H_2O} + (\dot{Q}_{sphtr} - \dot{Q}_{sld}) + W_{VAC}} \tag{6}$$

Where, $\dot{Q}_{red}$ is the heat requirement at the reduction reactor, $\dot{Q}_{oxd}$ is the heat released from the oxidation reactor. Since the OXI is an adiabatic reactor, $\dot{Q}_{oxd}$ would be zero. $\dot{Q}_{CO_2/H_2O}$ is

the net heat needed for the system operations, including the heat needed for heating up the sweep gas and the inlet $CO_2$ and/or $H_2O$ for splitting. $\dot{Q}_{sld}$ represents the heat recovered from the solids from the reduction reactor before it enters oxidation, while $\dot{Q}_{spht}$ is the heat delivered to the solids for preheating. However, in the present layout, no pre-heating was employed and hence would be equal to zero as well. Heat losses from system components were neglected in the efficiency assessment. Finally, $W_{VAC}$ represents the pumping work resulting from vacuum generation and removal of generated oxygen from the reduction reactor.

# 3 System Evaluation

To perform the necessary system evaluation of the proposed SCLP-OXY-CC unit, the metal oxide flow rate was first fixed. As explained before, for the base case add-on unit, 66 mol/s of gas ($CO_2$ and/or $H_2O$) was utilized. This would ideally require 66 mol/s of equivalent $Ce_2O_3$ flow into the oxidation reactor. However, considering a 20% excess gas flow in the oxidation reactor based on the sensitivity studies were chosen, and the corresponding maximum non-stoichiometry of 0.198 at a reduction temperature and pressure of 1600$^oC$ and $10^{-7}$ bar respectively, a $CeO_2$ recirculation rate of 275 mol/s in the CL unit was fixed.

Indeed, the value closely follows the mole flow of $CeO_2$ used for the previous sensitivity analysis. Additionally, the temperature range within which the proposed add-on unit was analysed was 1300 and 1600$^oC$, to obtain a considerable reduction extent. The reduction reactor volume of 0.5 $m^3$ was selected to minimize the heat requirement for the reduction by avoiding unnecessary heating of a large volume of the reactor without significant reaction. Also, this would ensure predicting well the heat requirement for the reduction since ASPEN Plus reports the heat of reaction and not the heat supplied to the reactor. However, the

oxidation reactor volume needs to be decided separately due to a maximum reduction extent of 0.2 as opposed to 0.35 considered for the sensitivity studies. Additionally, the impact on the system performance is essential to be analysed. In this regard, a sensitivity analysis to decide upon the reactor volume was performed by comparing two extreme cases of water splitting and $CO_2$ splitting. The results are shown in Figure 4.

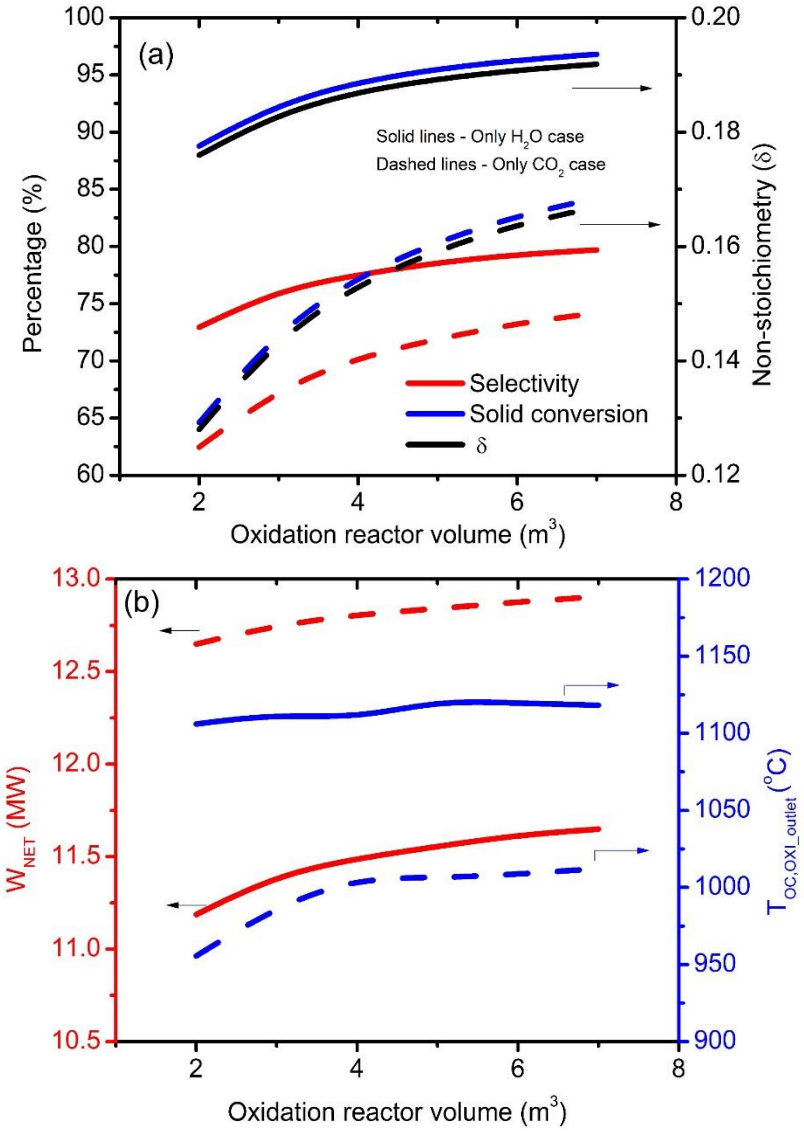


*Figure 4 Impact of the variation of the oxidation reactor volume with water splitting (Solid Lines) and $CO_2$ splitting (Dashed Lines) on the specific system performance of the proposed SCLP-OXY-CC add-on at a constant RED temperature and pressure of 1600°C and $10^{-7}$ bar respectively, a constant molar flow rate of $CeO_2$ and $CO_2/H_2O$ of 275 mol/s and 66 mol/s respectively, and a constant metal oxide and gas inlet temperature of 800°C to the OXI.*

The oxidation reactor volume was varied between 2 and 7 $m^3$. Due to the faster kinetics of water splitting, a reactor volume of 4 $m^3$ results in a minimum enhancement to the system performance. However, for a slower $CO_2$ splitting reaction, a larger reactor volume is required. Indeed, the highest impact of the variation of the reactor volume is seen on the solid conversion (metal oxide conversion), whereby for $CO_2$ splitting it increases from 65% for a 2 $m^3$ reactor to 80.4% for a 5 $m^3$ reactor and 84.2% for a 7 $m^3$ reactor. This also results in the net reduction extent in the redaction reactor (RED) to increase, due to a higher number of oxygen vacancies in the oxidized metal oxide. Nevertheless, besides the CL unit itself, a reactor volume of more than 5 $m^3$ is seen to have a lower impact on the overall system performance. While a rise of 0.2 MW of the net power production is noticed irrespective of the gas composition, the relative variation in the oxidized metal oxide outlet temperature from the oxidation reactor (OXI) is minimal beyond a reactor volume of 5 $m^3$. A combined effect of such variation of the system operating parameters results in a stable solar-to-electricity efficiency of the system of about 24.2% for working with the only $H_2O$ while the corresponding efficiency is 25.4% for only $CO_2$ splitting. Accordingly, 5 $m^3$ was selected as the reactor volume of the oxidation reactor (OXI). In the end, it can be claimed with confidence that such a conservative design would also ensure an operational flexibility with respect to available feedstock.

## 3.1 Sensitivity Analysis

To decide on the operating parameters and hence evaluate the achievable system efficiency, a comprehensive set of sensitivity was performed. The first set of sensitivity was performed to determine the impact of the inlet temperature of the gas and metal oxide into the oxidation reactor (OXI), all other parameters remaining constant. Following the discussions of the individual reactor sensitivity presented in [paper 1 reference], a minimal variation of the

system performance was noted with varying the gas inlet temperature to the OXI, irrespective of the gas composition. Irrespective of the gas composition, a net increase in the net power output of 0.5 MW is obtained for decreasing the gas inlet temperature from 1000$^{o}$C to 500$^{o}$C due to a decrease in the steam available for expansion in the steam turbine. However, with the rise in the gas inlet temperature, a rise in the metal oxide temperature at the OXI outlet is also observed, which would decrease the heat requirement for the same extent of reduction. Thus, no significant impact on system efficiency is obtained by varying the gas inlet temperature to the OXI, with an average efficiency of 24.2% and 25.4% being achieved for the only $CO_2$ and the only $H_2O$ cases respectively. Furthermore, for lower reduction temperatures, a gas inlet temperature beyond 800$^{o}$C would result in temperature cross-over between STEAMGEN and METHX-1 for water splitting, due to a higher heat requirement to evaporate water in comparison to sensible heat requirement for $CO_2$ heating. Hence, to ensure a flexible system operation irrespective of gas composition to the OXI, a gas inlet temperature of 800$^{o}$C was set.

Thereafter, by fixing the gas inlet temperature to the OXI at 800$^{o}$C, the reduced metal oxide temperature ($T_{OC,OXI\_inlet}$) to the OXI as varied between 600 and 1000$^{o}$C. A discussion on the variation in the individual power generation from the GT and ST, as well as the auxiliary power requirement, while working with either $CO_2$ or $H_2O$ is necessary. This can be followed from the results plotted in Fig 5b and c with varying the metal oxide inlet temperature to the OXI. A solid conversion ($X_{OXI}$) between 93% and 96.7% is noted between 600 and 1000$^{o}$C of $T_{OC,OXI\_inlet}$ for water splitting, while the corresponding values for $CO_2$ splitting yields and $X_{OXI}$ between 74.3% and 86%. This higher impact of $T_{OC,OXI\_inlet}$ on the $CO_2$ splitting reaction results in significant improvement to the reduction reaction as well for the only $CO_2$ case, whereby the non-stoichiometry ($\delta$) generated from reduction increases from 0.147 to 0.171. However, with a higher and a more constant solid conversion for water splitting, more

oxygen is available to be removed via reduction, resulting in the net δ generated to be improved from 0.184 at 600$^{o}$C to 0.191 at 1000$^{o}$C of $T_{OC,OXI\_inlet}$ (Fig 5c). For the same molar flow of gas to the OXI, a higher reduction extent in the RED results in a higher selectivity of $H_2$ (79.9% at $T_{OC,OXI\_inlet}$ 1000$^{o}$C) in comparison to the selectivity of CO (51.17% at $T_{OC,OXI\_inlet}$ 1000$^{o}$C), as can be seen from Fig 5b.

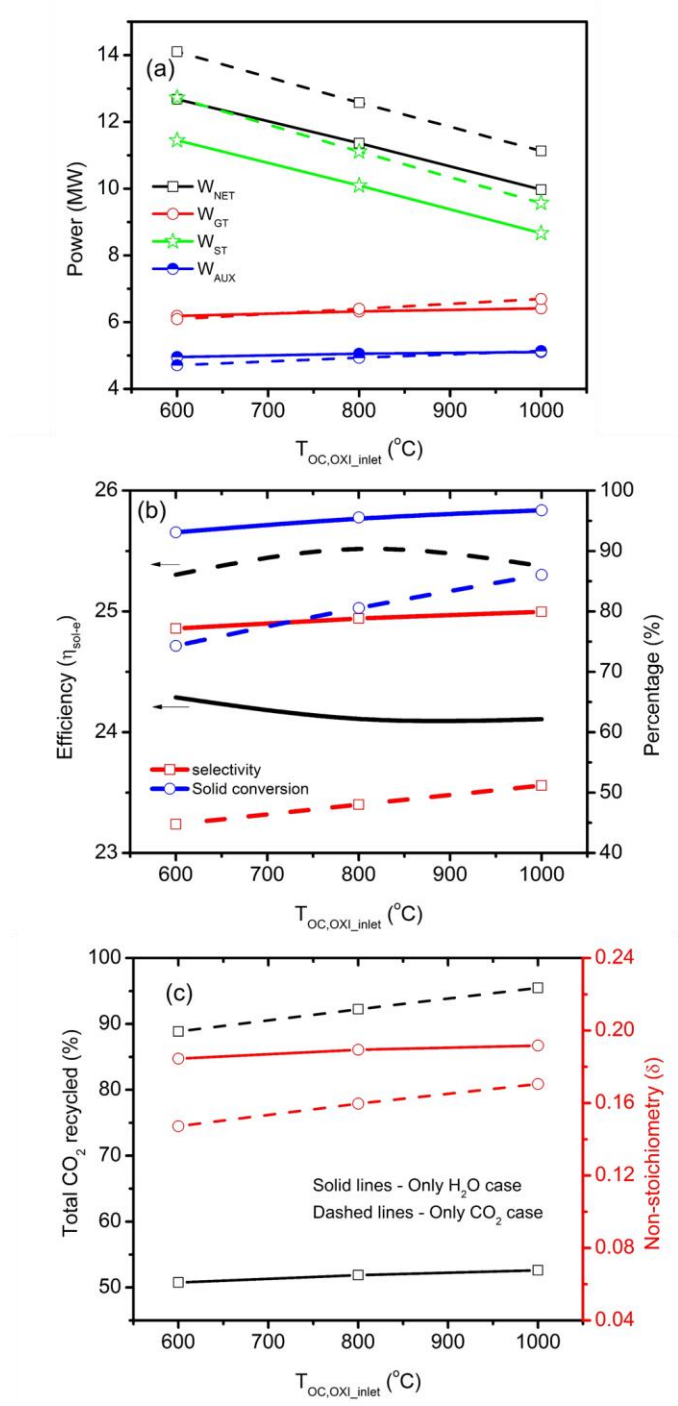


*Figure 3* Impact of the variation of the reduced metal inlet temperature to the OXI on the operating parameters of the SCLP-OXY-CC at a constant RED temperature and pressure of 1600ºC and $10^{-7}$ bar respectively, a constant molar flow rate of $CeO_2$ and gas to the OXI of 275 mol/s and 66 mol/s respectively and a constant gas inlet temperature to the OXI of 800ºC

Based on the selectivity, excess $CO_2$ is circulated to the combustion chamber to maintain the TIT at 1377$^o$C (1650K). For water splitting, the excess water is removed in the condenser before compression and combustion with recycled $CO_2$. For a lower variation in the selectivity of $H_2$, this results in similar molar flow to be expanded in the GT irrespective of $T_{OC,OXI\_inlet}$ . On the other hand, for $CO_2$ splitting the final $CO_2$ expanded is balanced by the recirculated carbon dioxide into the combustor. Hence, the GT output remains constant at 6.3 MW irrespective of the gas composition used for splitting. However, a higher heat is required to heat water from 25$^o$C to 800$^o$C than $CO_2$ due to the requirement of latent heat for the former. This would result in a lower heat availability in METHX-2 for steam generation causing a lower steam to be expanded in the steam turbine for the water only scenario. A drop of almost 1 MW drop in the power output from the ST is observed hence. As for the auxiliary power demand, no significant effect is noticed from the variation of the $T_{OC,OXI\_inlet}$. Therefore, a drop in the net electricity output from 14.1 MW to 11.1 MW is observed with increase in $T_{OC,OXI\_inlet}$ from 600$^o$C to 1000$^o$C for working with the only $CO_2$ with the corresponding output with only $H_2O$ being always about 1.2 MW lower.

A combined impact of the individual variations is obtained in the plant efficiency ($\eta_{sol-e}$). Indeed, to comment on the plant efficiency, the impact of the metal oxide and split gas temperature from the oxidation reactor is crucial to be considered as well. As can be followed from the previous sensitivity results, an increase in the $T_{OC,OXI\_inlet}$ significantly increases both the $T_{OC,OXI\_outlet}$ and the gas outlet temperature from the OXI. While the former decreases the thermal requirement in the RED, the cooling of the gas from higher temperature results in a larger steam generation. Indeed, the exothermicity of water splitting is higher, a higher temperature of both metal oxide and the product gas from the OXI is obtained for water splitting than with $CO_2$ splitting. Thus, a constant lower heat (around 1.5 MW) would be

required in the RED to maintain the temperature while working with only water as opposed to that while working with the only $CO_2$. Notwithstanding this fact, due to a relatively higher net electricity output, the overall efficiency for a pure $CO_2$ operated SCLP-OXY-CC unit is higher by one percentage point than for a pure water operating cycle. Based on the relative impact of all the parametric variations resulting from the variation of the $T_{OC,OXI\_inlet,}$ an optimum efficiency is reached (25.5%) at 800$^oC$ of $T_{OC,OXI\_inlet}$ for $CO_2$ only operation (Fig 5b).

A variation in the reduction temperature between 1300 and 1600$^oC$ was performed and its impact on the system performance was evaluated. Similar logical reasoning can be followed from the discussions of the previous sections. A lower reduction temperature results in a lower non-stoichiometry (δ), which significantly increases with temperature (Fig 6a). A constant molar flow in the OXI would therefore significantly decrease the selectivity of the product gas in the OXI. So much so, that for $CO_2$ splitting with no separation of the product and reactant gas, the TIT would not be possible to be maintained for a constant molar feed rate of gas to the OXI from around a RED temperature of 1400$^oC$. This is shown in Fig 6b, whereby the molar flow sent to the OXI corresponds to only 15% and 2.5% of the total $CO_2$ molar flow sent for CCS from the original Oxyfuel power plant. This, however, results in the selectivity of CO to increase at 1300$^oC$ from that of 1400$^oC$ of reduction temperature. On the other hand, even though the $H_2$ selectivity drops to almost around 2%, the presence of the condenser ensures a stable TIT to be maintained by varying the flow of the recycled $CO_2$ in the combustor accordingly. Nevertheless, with the decrease in the production of $H_2$ with reduction temperature, the overall $CO_2$ recycled would drop as well from around 52% at $T_{RED}$ of 1600$^oC$ to lower than 2% for a $T_{RED}$ of 1300$^oC$, as shown in Fig 6c. A maximum $CO_2$ recycling rate of about 65% is obtained for working with the only $CO_2$ at a reduction temperature of 1600$^oC$.

As can be followed from the kinetic discussions, a lower non-stoichiometry in the reduction reactor would also significantly decrease the reaction rate of the oxidation reaction. Due to slower kinetics resulting from a smaller number of vacancies in the reduced metal oxide, the solid conversion drops as well with a decrease in the reduction temperature. This effect can be seen in Fig 6b as blue coloured lines. The solid conversion with water splitting is inherently higher than that with $CO_2$ splitting, yielding a conversion of over 96% at $T_{RED}$ of 1600$^{o}$C, while the corresponding value with $CO_2$ splitting is 80%. Indeed, it needs to be clarified that a higher solid conversion fraction does not imply a higher $H_2$ or CO generation since the conversion fraction essentially indicates the relative change in the oxidation state of the ceria between the inlet and outlet of the reduction reactor, irrespective of the absolute value of $\delta$ generated.

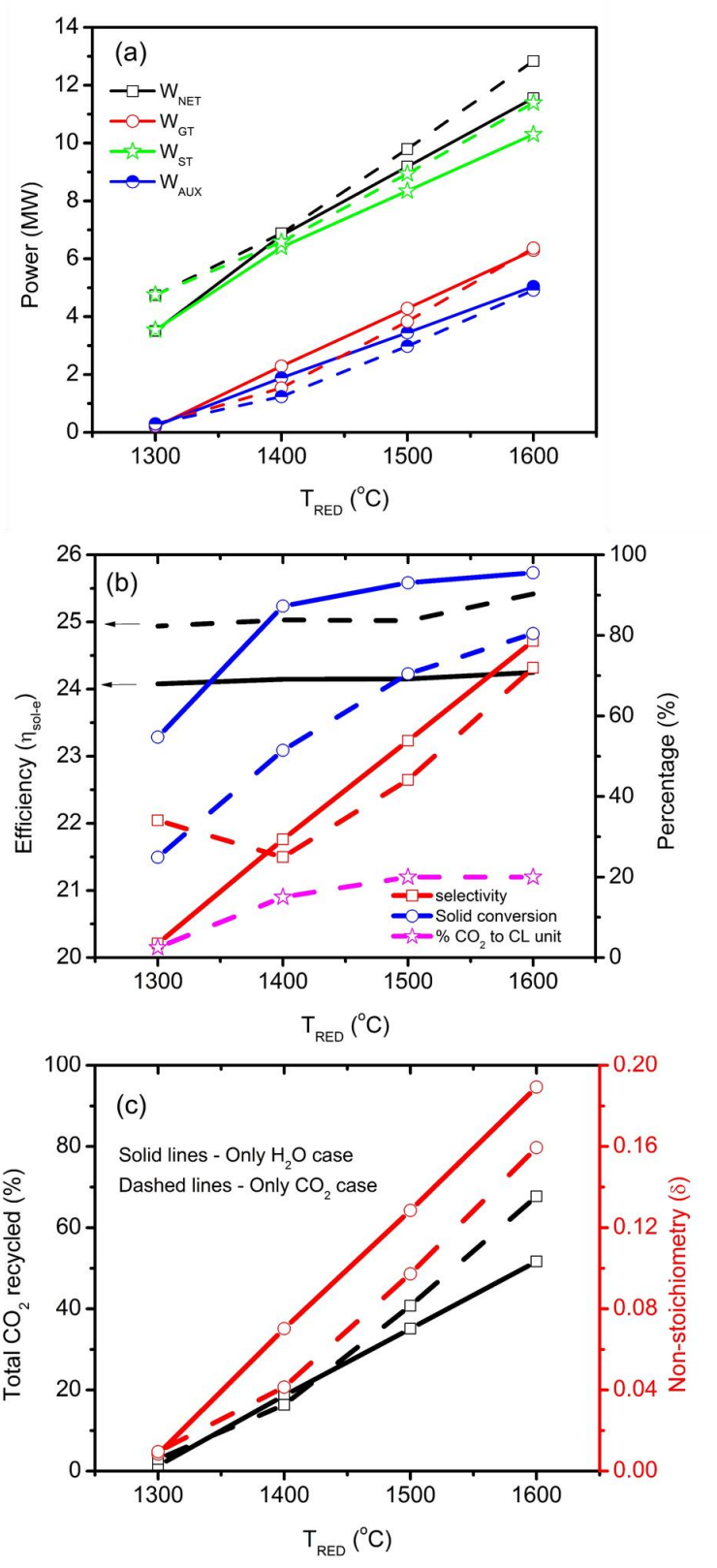


*Figure 6* Impact of the variation of the reduction temperature on the operating parameters of the SCLP-OXY-CC at a constant RED temperature and pressure of 1600ºC and $10^{-7}$ bar respectively, a constant molar flow rate of $CeO_2$ and gas to the OXI of 275 mol/s and 66 mol/s respectively and a constant gas inlet temperature to the OXI of 800ºC

The impact of the absolute amount of $H_2$ or CO generated in the OXI, directly proportional to the net non-stoichiometry generated in the RED can be visualized through the relative power outputs from the GT and ST and the auxiliary consumptions within the proposed unit. A higher δ at a higher $T_{RED}$, results in higher $H_2$ and CO yield, leading to a higher power output from the GT, the maximum being around 6.3 MW. On the other hand, a higher $T_{RED}$ leads to greater heat availability and steam generation from MET-HX2, increasing the output from the ST as well. The power of the ST in only water cycle is lower due to reasons already discussed previously. The auxiliary power requirement is primarily due to the $CO_2$ recycle compressor and product gas compressors necessary prior to the combustor. Additional power needs for ASU operation and pump work are, however, much smaller in the proposed plant design. Therefore, with the drop in the overall $CO_2$ recycled in the add-on unit, as well as for less product gas generated with a drop in the temperature of reduction, the auxiliary power requirement drops as well for a lower $T_{RED}$. A combined effect is seen on the net power output from the system, whereby only around 4.5 MW of electric power output is achieved at a TRED of 1300$^o$C irrespective of gas composition for the OXI. However, for a higher $T_{RED}$ resulting in greater solid conversion, together with a higher power requirement for hydrogen compression than CO compression, and a corresponding lower output from the ST, the net power output from the $H_2O$ only cycle is lower. At a $T_{RED}$ of 1600$^o$C, thus, around 11.6 MW of electric power is obtained, compared to 12.8 MW from the $CO_2$ only cycle (Fig 6a).

Indeed, similar to the discussions and conclusion of the previous sensitivity analysis, the impact of $T_{RED}$ on the efficiency of the power plant is shown in Fig 6b. No notable change in the efficiency is seen for a cycle operating with only $H_2O$, whereby the efficiency remains constant at around 24.2%. On the other hand, a maximum efficiency of 25.4% is obtained with only $CO_2$ and $T_{RED}$ of 1600$^o$C, which becomes constant at 25% below a $T_{RED}$ of 1500$^o$C.

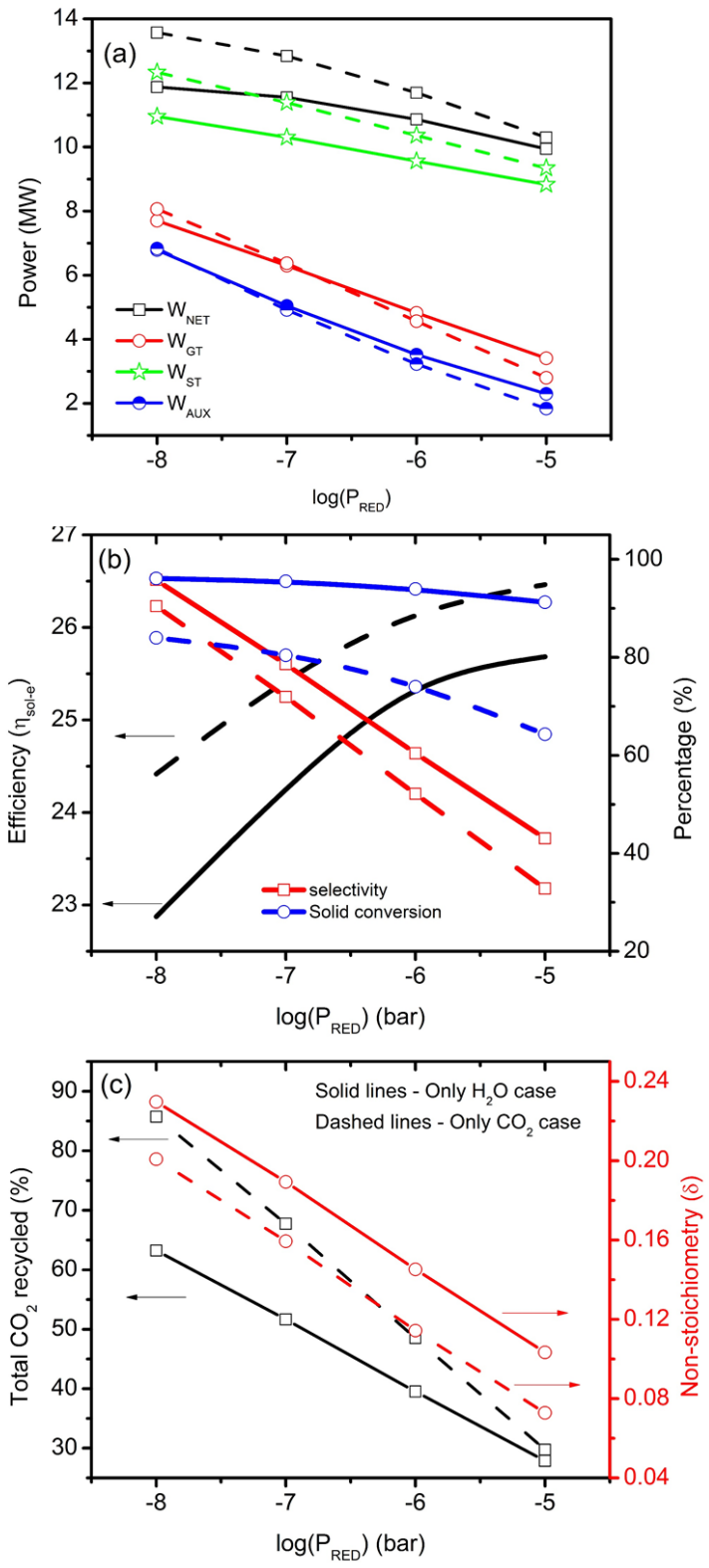


*Figure 7* Impact of the variation of the reduction vacuum pressure on the operating parameters of the proposed SCLP-OXY-CC add-on unit at a constant RED temperature of 1600ºC, a constant molar flow rate of $CeO_2$ and gas of 275 mol/s and 66 mol/s respectively and a constant gas and metal oxide inlet temperature to the OXI of 800ºC.

The impact of the variation of the reduction vacuum pressure is shown in the following Fig 7. Similar to the variation of the $T_{RED}$, a higher vacuum pressure increases the system yield significantly, in terms of the generated non-stoichiometry, as well as the selectivity for a constant molar flow of the gas to the OXI. As discussed before, due to a lower solid conversion in the OXI from $CO_2$ splitting, the resulting $\delta$ in the RED for the $CO_2$ only cycle is lower by about an average of 0.03. The corresponding selectivity of CO is also lower by 5 to 10% compared to that of $H_2$, which varies between 43% to 95.8% at reduction vacuum pressure of $10^{-5}$ and $10^{-8}$ bar respectively.

A higher selectivity would hence imply a higher net $CO_2$ recirculation within the add-on unit, which is indeed the case, as shown in Fig 7c. For lower vacuum conditions of the $10^{-5}$ bar, the selectivity of the CO generated is lower, requiring around 10% of the total flow of $CO_2$ to be recirculated in the combustor while maintaining the desired TIT. The net $CO_2$ recycled was then 30% (20% $CO_2$ being sent previously directly to the OXI). As for operating with $H_2O$, around 30% of $CO_2$ is necessary to ensure the desired TIT with $H_2$ combustion. Nonetheless, for higher vacuum pressures and with an increase in the selectivity, the overall $CO_2$ circulated in the add-on unit increases, whereby a maximum recirculation of 85.7% is seen at a pressure of $10^{-8}$ bar. The corresponding value at $10^{-7}$ bar was 51.7% and 67.7% for working with only water and $CO_2$ respectively.

Similar trends in the power generation from the GT and the ST, together with the auxiliary power requirement and the net power produced in the add-on unit as was previously seen by varying $T_{RED,}$ is shown in Fig 7a. Besides all previous discussions, it is important to mention that a higher vacuum pressure, even though would ensure a higher reduction extent of ceria, and hence a higher selectivity, for a constant reactant gas molar flow, would also result in an increased auxiliary consumption from vacuum pumping. Also, the heat of reaction increases

with reduction extent, requiring more heat to be supplied. These factors, therefore, offset the net gains of the productivity of OXI and hence an increased power output from the proposed layout at increased vacuum conditions of reduction. Thus, even though a decrease in the operating pressure of the RED from $10^{-7}$ bar to $10^{-8}$ bar operation would increase the $W_{NET}$ by 0.3 to 0.7 MW (for $H_2O$ and $CO_2$ respectively), the net system efficiency drops by over 1% in both the cases (Fig 7b). Hence a trade-off in the reduction pressure with respect to system optimization is necessary for the proposed add-on unit.

The impact of the quantity of water and $CO_2$ into the OXI for a constant ceria recirculation rate was performed subsequently. A reduction temperature of 1600$^o$C with a metal and gas inlet temperature of 800$^o$C was fixed. Indeed, interesting to note is the maximum flow of water that can be utilized within the plant without temperature cross-over. Though not shown explicitly in Fig 8, it can be understood that a maximum of around 42% of the available water (230 mol/s) could be utilized at the set temperature configuration of the system. This would allow scale-up of the system further.

Nevertheless, as can be seen from the Fig 8a, around 10% of the flow (55 mol/sec) corresponds to the stoichiometric amount of water necessary to oxidize the non-stoichiometry of Ceria. Below this, a sub-stoichiometric flow would cause an incomplete reaction in the oxidation reactor, and hence significantly diminish the system effectiveness, as well as the efficiency. Beyond the stoichiometric flow (10% of $H_2O$ from the CCS unit), the selectivity of hydrogen drops due to stoichiometrically excess flow, however, without any significant benefit to the solid conversion, and hence subsequently, the reduction extent, $\delta$, of the oxidized metal (Fig 8a). By increasing the fraction of $H_2O$ to CL, a peak oxidized metal outlet temperature from the OXI ($T_{OC\_OUT,\ OXI}$) of 1120$^o$C at around stoichiometric flow rates. Indeed, it needs to be mentioned that unlike the sensitivity study, where a $\delta$ of 0.35 was

assumed at the OXI inlet, in the present layout, the δ is 0.198. Hence, a much lower temperature of both the gas and the metal oxide from the outlet of the OXI is obtained. This considerably limits the overall performance of the CL unit while operating in a closed cycle. Nevertheless, at lower flow fraction of $H_2O$, the product outlet temperature (both gas and metal) is lower due to unreacted metal, while at higher flow, the cooling from the excess gas flow, lowers the metal oxide outlet temperature. However, with a higher flow rate, due to be a counterflow reactor, a paradigm difference in the temperature of the gas outlet at the OXI is noticed, a rise in almost 150°C between before and after the stoichiometry flow respectively (Fig 8c).

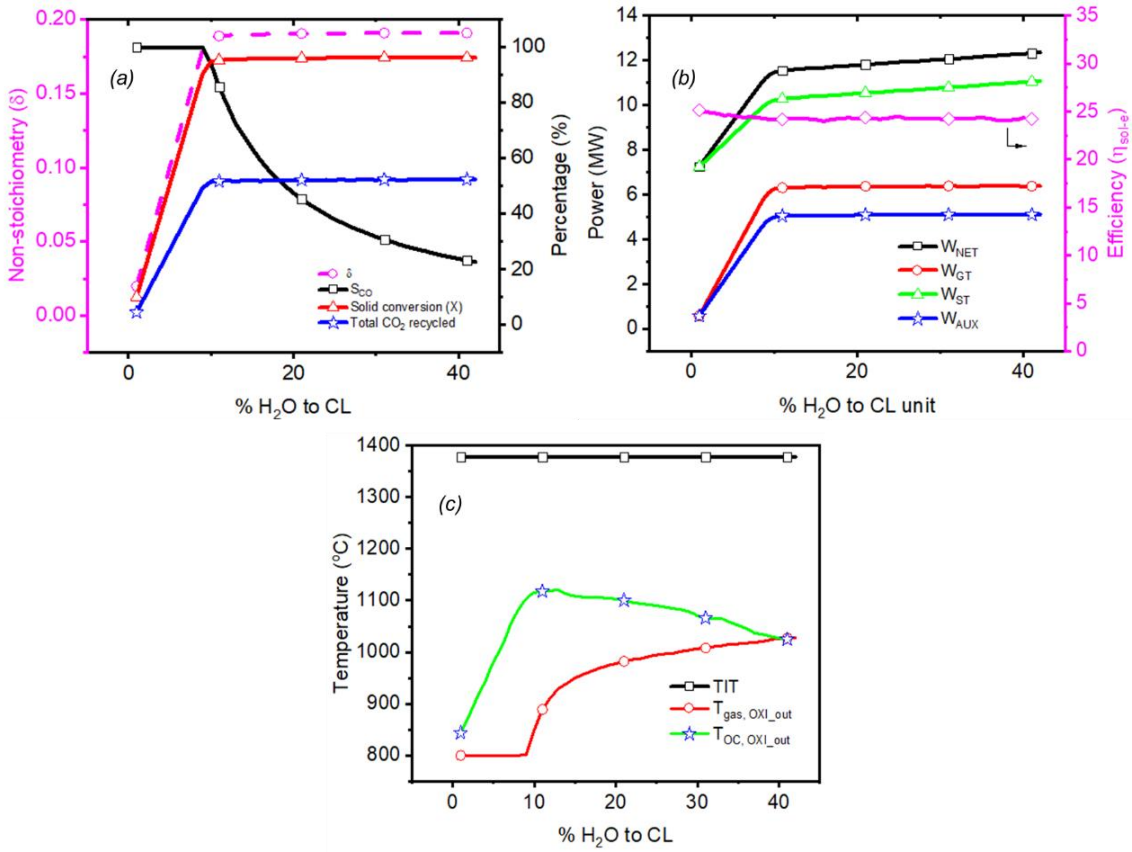


*Figure 8*. Impact of the variation of the water flow rate (% $H_2O$ to CL) on the parameters of the proposed SCLP-OXY-CC unit working with only water at a constant molar flow rate of $CeO_2$ and water of 120 mol/s, a constant gas and metal inlet temperature of 800°C to the OXI and a constant reduction temperature and pressure of 1600°C and $10^{-7}$ bar

Being limited by the molar flow of metal in the OXI for a constant molar flow of $CeO_2$, the molar flow of hydrogen generated beyond 10% of $H_2O$ from CCS exhaust to the CL unit becomes constant. The moisture being separated, this results in a constant molar flow of hydrogen and hence a constant GT power of 6.3 MW beyond 10% of $H_2O$ to CL in the proposed add-on SCLP-OXY-CC power plant. The TIT could also be maintained constantly at 1377$^oC$, as can be followed from Fig 8c.

However, since a higher amount of steam is sent for splitting, a larger heat content in the gas from the OXI results in the generation of more steam from cooling a higher volume of gas, which subsequently increases the power output from the steam turbine. The auxiliary power need being almost constant (Notwithstanding the minimal power increase from pumping additional water), the net power output from the system increases up to 12.35 MW for an $H_2O$ to CL fraction of 0.42. Nevertheless, an increase in the heat requirement in RED from lowering the metal inlet temperature to the RED by passing excess steam in the OXI results in no net benefit to the system efficiency beyond 10% of $H_2O$ to CL. A maximum average system efficiency with water at the proposed operating conditions can hence be said to be 24.2% as seen in Fig 8b interestingly such excess flows would often be limited to operating power cycles only, which do not require a high purity product gas from the OXI. For chemical processes like Fischer-Trophs synthesis, the need for high purity product would limit the excess of steam into the OXI reactor to around 5% excess to the stoichiometry and hence, a limit of the attainable system performance.

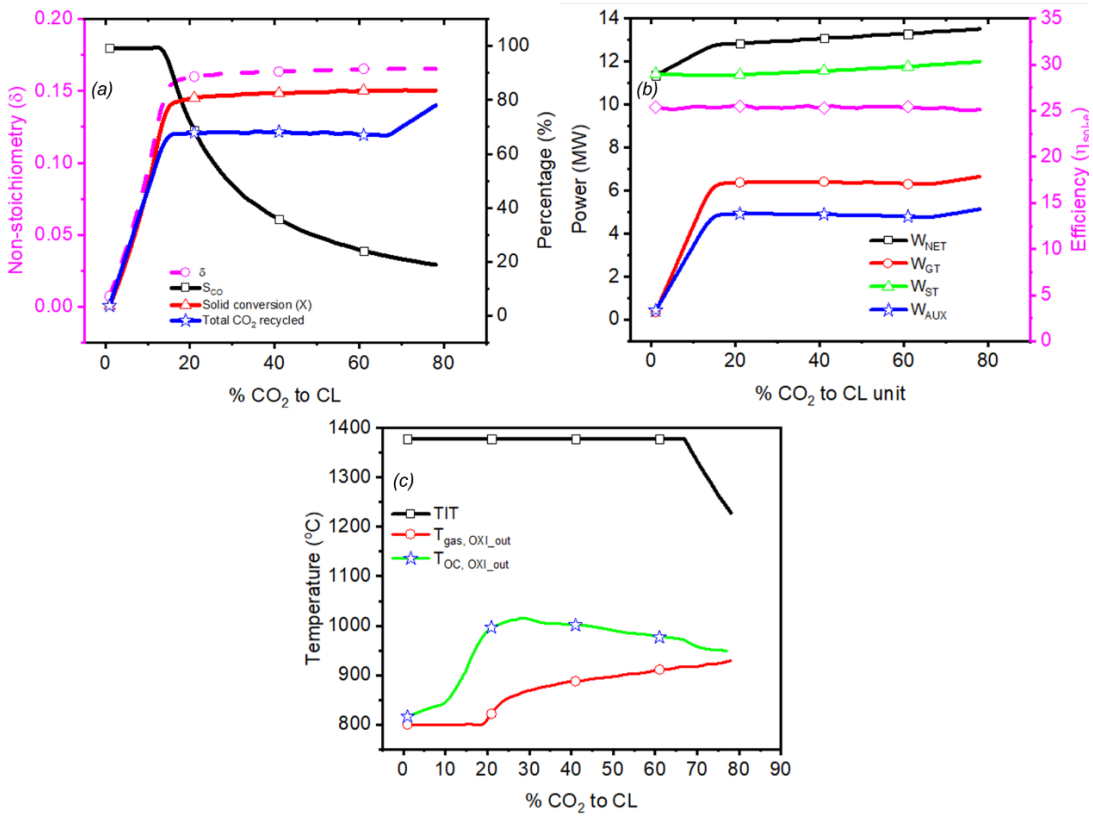


*Figure 9*. Impact of the variation of the $CO_2$ flow rate (% $CO_2$ to CL) on the parameters of the proposed SCLP-OXY-CC unit working with only water at a constant molar flow rate of $CeO_2$ and water of 120 mol/s, a constant gas and metal inlet temperature of 800°C to the OXI and a constant reduction temperature and pressure of 1600°C and $10^{-7}$ bar

On the other end, the impact of the variation of the $CO_2$ flow into the CL unit on the different system operating parameters, together with the individual outputs of the turbine, as well as the auxiliary power input to the system and the net system efficiency is plotted in Fig 9. The reduction temperature was fixed at 1600°C, together with the gas and reduced metal oxide inlet temperature to the OXI at 800°C. No temperature cross-over was noticed until a 78% recycling fraction of the $CO_2$ to the CL unit. This is since, unlike water, no phase change of $CO_2$ takes place, and hence the sensible heat required to heat up the $CO_2$ is much lower.

Similar profiles to that of only water splitting are observed in all the cases. At around 16.7% of the $CO_2$ fraction to the CL unit, which corresponds to the stoichiometric flow, a complete conversion of the gas (Fig 9a), together with a stable solid conversion of 83% is obtained.

Being an exothermic reaction, this also results in the highest output temperature to the metal oxide from the OXI, around 1020$^{o}$C, about 100$^{o}$C lower than the maximum temperature achieved in water splitting. All the related arguments of obtaining a lower temperature are valid for $CO_2$ as well and hence not discussed separately. However, the gas outlet temperature rises gradually, being a counterflow reactor. However, no significant benefit is gained, since the metal oxide outlet temperature drops, signalling a higher thermal requirement in the reduction reactor. Due to a high conversion rate in the OXI for the gas at stoichiometry, the corresponding requirement of the $CO_2$ in the combustor for maintaining the TIT also peaks at 15% of $CO_2$ to CL unit, (not shown). With a further rise in the $CO_2$ fraction to CL, the selectivity starts to drop lower, and beyond 65%, the excess $CO_2$ in the product gas results in a drop in TIT without additional need of $CO_2$ to be recycled, as can be seen in Fig 9c.

Fig 9b shows the net power output, together with the outputs from the GT and the ST and auxiliary power requirements with the variation of the $CO_2$ flow to the splitting unit. As can be seen, after the 16% $CO_2$ from the CCS stream to CL, the GT power remains constant, since the total gas expanded is constant following previous arguments. However, with a higher flow of the $CO_2$ to the CL unit, and with a rise in temperature of the outlet gas from the OXI, as seen in Fig 9a, the net steam generation increases, resulting in the increase of the net power output from the system. Beyond the 65% of $CO_2$ to CL, the net gas compressed for the COMB increases to a limit that decreases the TIT. This results in a steady rise in the auxiliary power demand. Even though the TIT decreases, the gas turbine sees a slight increase in power output due to the expansion of a larger volume of gas. The ST power increases, however, at a lower rate, since the temperature of the GT exhaust decreases, even though the net volume of the gas flow increase. Combining all these factors, a linear increase in the net power output from the system is noticed beyond 65% fraction of the $CO_2$ to CL

unit. However, due to the lowering in the metal oxide outlet temperature from the OXI, leading to an increased heat load in the RED, the net system efficiency remains unaffected throughout at around 25.4%, as can be seen in Fig 9b.

# 4 Comparative Evaluation

A comparative evaluation of the performance of the proposed SCLP-OXY-CC add-on unit by utilizing three different gas mixtures (only $CO_2$, only $H_2O$ and 86% $CO_2$ and 14% $H_2O$ as replication of the composition of an Oxyfuel NGCC exhaust) was performed, fixing the operating conditions, based on the above sensitivity analyses. The reduction reactor temperature and operating pressure were chosen as a 1600$^oC$ and $10^{-7}$ bar, together with the metal oxide and gas inlet temperature to the OXI at 800$^oC$. Since the primary aim of the proposed layout was power generation, the net molar flow of the gas was kept constant at 66 mol/s (equivalent to the utilization of 20% of $CO_2$). With regards to the product gas, no limit to the purity of the gas produced in the OXI is necessary as it will be fed to the combustor for power generation.

Table 2 Comparative performance evaluation of the proposed SCLP-OXY- CC, add-on unit with varying gas compositions to the OXI at equivalent operating conditions of 1600$^oC$ and $10^{-7}$ bar reduction temperature and pressure respectively, metal and gas inlet temperature to the OXI of 800$^oC$, 275 mol/s flow of $CeO_2$ and gas flow to the OXI of 66 mol/s

| Plant data | Units | Only $CO_2$ | 86% $CO_2$, 14% $H_2O$ | Only $H_2O$ |
|---|---|---|---|---|
| Solar Energy Input (A) | MWth | 33.72 | 31.76 | 31.81 |
| Net GT Output | MWe | 6.30 | 6.30 | 6.30 |
| ST Output | MWe | 11.380 | 10.512 | 10.30 |
| Gross Electric Power Output (B) | MWe | 17.68 | 16.812 | 16.596 |
| ASU Consumption + $O_2$ compression | MWe | 0.024 | 0.024 | 0.024 |
| Recycled $CO_2$ Compression | MWe | 1.754 | 1.659 | 1.877 |
| Compressor/ Pump Work for OXI Feed | MWe | 0.324 | 0.319 | 0.353 |
| Power Cycle Pumps | MWe | 0.130 | 0.119 | 0.117 |
| Syngas Compressors | MWe | 0.562 | 0.552 | 0.455 |

| | | | | |
|---|---|---|---|---|
| Vacuum Pump | MWe | 2.033 | 1.997 | 2.216 |
| Total Auxiliary Power Consumption (C) | MWe | 4.827 | 4.67 | 5.041 |
| Net Electrical Power Output (D=B-C) | MWe | 12.853 | 12.142 | 11.555 |
| Gross Electrical Efficiency (B/A*100) | % | 52.43% | 52.93% | 52.17% |
| Net Electrical Efficiency (excluding solar field and receiver efficiency) (D/A*100) | % | 38.12% | 38.23% | 36.32% |
| Net System Efficiency (Solar to Electricity) | % | 25.44% | 25.52% | 24.25% |
| Non-Stoichiometry yield (δ) | | 0.1652 | 0.1706 | 0.1893 |
| Metal oxide Inlet Temperature to RED | $^{o}$C | 1006.17 | 1032.26 | 1121.36 |
| Metal oxide Conversion in the OXI | % | 80.43 | 86.09 | 95.53 |

The above table 2 lists the comparative plant performance of the proposed SCLP-OXY-CC add-on unit with the three different gas mixtures discussed above. As can be observed, working with only water forms the lower bound to the system performance, while that with $CO_2$ provides the upper bound to the system performance in terms of the solar to electricity efficiency of the proposed add-on unit.

From the previous discussions, even though the power generated in the gas turbine is almost constant irrespective of the gas composition, the steam turbine output decreases significantly with increased water content in the gas mixture to the OXI. Additionally, a higher vacuum pumping power is necessary due to a higher yield of non-stoichiometry for $H_2O$ splitting, which significantly increases the overall auxiliary power requirement as well. Even though this results in a higher yield of product from the system, indicated by a higher non-stoichiometry obtained by working with only water, as compared to working with $CO_2$/ $CO_2$-$H_2O$ mixture. Furthermore, a higher temperature solid outlet temperature from water splitting would result in the net heat required for reduction to decrease, which is a significant benefit of increasing the amount of water in the gas mixture to the OXI. Also, the solid conversion increases significantly with the increase in water content of the mixture, whereby, even with

14% water content, a 5.5% increase in the solid conversion is noticed, while the corresponding increase is 15% between working with only $CO_2$ and only $H_2O$.

Indeed, a maximum thermal efficiency of 38.12% of the proposed layout is obtained while working with only $CO_2$ splitting. This also provides simplest of configurations, without the need of HRSG for steam generation for splitting and additional condensers for water removal from different streams of the power plant. Nevertheless, the overall solar-to-electricity efficiency drops to 25.4% due to the efficiency penalties arising from the solar field losses and losses in the receiver, which, in fact, is the heat inlet to the reduction reactor. The maximum net electricity yield of 12.9 MW is obtained correspondingly.

Table 3 Comparative performance evaluation of the proposed CL unit of the proposed SCLP-OXY-CC with varying gas composition to the OXI at equivalent operating conditions of 1600ºC and $10^{-7}$ bar reduction temperature and pressure respectively, metal and gas inlet temperature to the OXI of 800ºC, 275 mol/s flow of $CeO_2$ and gas flow to the OXI of 66 mol/s

| Description | Only $CO_2$ | 86% $CO_2$, 14% $H_2O$ | Only $H_2O$ |
|---|---|---|---|
| Solar Energy Input (A) | 33.72 | 31.76 | 31.81 |
| $H_2$ Flow (mol/s) | 0 | 8.946 | 51.8116 |
| CO Flow (mol/s) | 47.469 | 37.955 | 0 |
| Energy yield rate (MW) | 13.481196 | 12.854692 | 12.020291 |
| Vacuum pump work in RED (MW) | 2.033 | 1.997 | 2.21591 |
| Heat Need for $CO_2$/$H_2O$ Heating (MW) | 2.329 | 2.7 | 4.947 |
| Efficiency of CL Unit ($\eta_{SCL}$) | 35.41% | 35.26% | 30.84% |

In addition to evaluation of the solar to electricity efficiency of the entire layout, the efficiency of the CL unit alone is also of interest. The corresponding evaluation results are shown in the following table 3. As can be seen, at similar operating conditions, due to a higher metal oxide inlet temperature to the RED, the solar energy input for operating with only water is the minimum. However, due to latent heat requirement in heating water, the heat need for the water heating is significantly higher than the corresponding for $CO_2$, by more than 2.5 MW. In addition, a higher $\delta$ with water results in an increased requirement of

vacuum pump work to maintain the necessary vacuum pressure in he reduction reactor. Thus, similar to the trend of results obtained for the overall plant efficiency, the efficiency of the CL unit decreases proportionally with increased water content in the gas mixture to the OXI as well. A maximum CL unit efficiency without considering heat recuperation is therefore obtained as 35.4% while working with only $CO_2$.

## 4.1 Comments and Discussions

A comprehensive evaluation of the proposed SCLP-OXY-CC add-on unit was performed varying not only multiple operating conditions, but also the gas composition to the OXI. Based on such analyses, operation strategies and concerns with two extreme mixture compositions (only $CO_2$ and only $H_2O$) have been described and evaluated. The net efficiency obtained was found to vary between 24.5% and 25.7%. This can however, be sought to be increased via further system optimization. The net power generated was correspondingly found to be between 11.5 and 12.9 MW with the add-on unit. Considering the solar energy to be free, the power generation from the combined 100MW CCS and the SCLP-OXY-CC add-on unit would result in a maximum net system efficiency of about 49.7%, a 5.7% rise to the original efficiency of 44% of the Oxyfuel with CCS unit, as described above. Besides, the variability in the power output, without a significant drop in the system efficiency would aid flexible operations with the necessary control system. However, a significant drop in the power output at low reduction reactor temperature would often limit the operation of the cycle throughout the day without integrating adequate storage. This becomes increasingly more significant since at start-up conditions, occurring every day, a temperature of 1600$^{o}$C could seldom be reached. This would, therefore, limit the system performance to achieve its maximum potential only during a few hours around mid-day.

Thus, a further complex system design with the integration of storage would be necessary for the resilient operation of the proposed layout.

# 5 Economic Evaluation

## 5.1 Methodology

Further to the technical assessment of the system, economic assessment is crucial as well to comment on the overall feasibility of the proposed layout. Capital cost (including specific investment costs), Operational and Maintenance (O&M) costs and levelized cost of electricity (LCOE) were considered as the primary economic indicators to the proposed SCLP-OXY-CC system. The costs of the different components were obtained from literature, either directly, or after suitable assumptions. In this regard, the costs were updated for present day through chemical plant cost indices [32]. Besides, a currency conversion factor of 1.23 USD/EUR was used.

The Capital cost of the plant (CAPEX), included the capital cost of each module or equipment and was estimated by utilization of the component scaling factor exponent, which is shown as the following equation

$$C_E = C_B \times (G / G_{ref})^M \quad (7)$$

$C_E$ and $C_B$ representing the equipment cost with a capacity of G and $G_{ref}$, respectively; M is the equipment scaling factor exponent, ranging between 0.6 – 1 [33,34]. The summary of the scale factors for the different components of the plant can be found in Farooqui et al [27] and scaling factor for solar tower and its component with reflectors are considered as unity.

To assess costs beyond equipment costs, that is, costs associated with plant installation and other direct and indirect costs related to the project development, a bottom-up approach [34] was used and is summarized in Table 4.

The *Total Equipment Cost (TEC)* is the sum of all module costs in the plant. Besides this, additional *installation costs* are incurred due to expenses being required while integrating the individual modules into the entire plant, comprising costs for piping or valves, civil works, instrumentations, electrical installations, insulations, paintings, steel structures, erections and other outside battery limit (OSBL) activities.

*Total Direct Plant Cost (TDPC)* is then calculated as the sum of the Module/Equipment Costs and the Installation Costs. *Indirect Costs* have been fixed to 14% of the TDPC for all the three technologies [34], which include the costs for the yard improvement, service facilities and engineering costs as well as the building and sundries.

*Engineering, Procurement and Construction Costs (EPC)* was calculated as the sum of the Total Direct Plant Cost and Indirect Costs. Finally, the *Owner's Costs and Contingencies* (OCC) were included as the owner's costs for planning, designing and commissioning the plant and for working capital, together with contingencies, and were fixed to 15% of the total EPC cost for all the technology options as per literature [34]. In addition, the cost of initial metal oxide loading was also accounted for, which led to the overall CAPEX or *Total Plant Cost (TPC)* of the project to be obtained as per the following equation.

$$\text{TPC} = \text{EC} + \text{Installation Costs} + \text{Indirect Costs} + \text{OCC} + \text{Metal oxide Loading Costs} \quad (8)$$

In parallel, the O&M costs mainly comprise two aspects, namely fixed O&M costs and variable O&M costs. Fixed O&M costs comprise five components, i.e. general annual maintenance cost including overhead cost, property taxes and insurance and direct labour cost. On the other hand, variable costs are connected with the costs associated with power generation, include the cost of water (including both process water and make-up water), cost of a metal oxide for make-up, and fuel costs [34]. In the present calculation, solar energy was assumed to be available for free and no fuel cost was considered.

Table 5 presents the basic parameters used for calculating economic indicators of the proposed power plant including those discussed in the previous sections. Based on the literature, erected cost of most of the equipment was obtained [35]. However, for the rest, the erection, piping and other added costs were considered as per the following table 5.

Table 1 Basic economic assumptions [34,36,37]

| Item | Assumption |
|---|---|
| Ceria oxide price | 49 $/kg |
| Process Water | 7.43 $/m$^3$ |
| Make-up Water | 0.43 $/m$^3$ |
| Erection, Steel structures and Painting | 49% of Equipment Cost |
| Instrumentation and Controls | 9% of Equipment Cost |
| Piping | 20% of Equipment Cost |
| Electrical Equipment and Materials | 12% of Equipment Cost |
| Indirect Costs, including Yard Development, Building, etc. | 14% of TDPC |
| Owner's Costs | 5% of EPC |
| Contingencies | 10% of EPC |
| Annual operational time | 1862 hours |
| Property Taxes and Insurance | 2% of TPC |
| Maintenance Cost | 2.5% of TPC |
| Labour Cost (Million Euro) | $100 per kW |
| Operational Life of Plant | 30 years |
| Interest Rate | 10% |
| Carbon Tax | None of the base case evaluation |
| Electricity Price | 50 $/MWh |

The levelized cost of electricity (LCOE) was considered to assess the economic performance of the system, where, the "break-even" value for producing a unit of electricity is often employed as a parameter to compare different electricity production technologies from the economic point of view. The LCOE is expressed as the following expression (equation 22),

based on the investment cost at time period t ($I_t$), O&M Costs at time period t ($M_t$), Fuel Cost at time period t ($F_t$), the electricity generated at time t ($E_t$) and the interest rate r.

$$\mathrm{LCOE} = \frac{\sum \frac{I_t + M_t + F_t}{(1+r)^t}}{\sum \frac{E_t}{(1+r)^t}} \quad (9)$$

## 5.2 Capital Cost and Operational Expenses

As developed from the process simulations, it can be easily concluded that the SCLP-OXY-CC provides a clear technical benefit to a conventional oxyfuel NGCC system with carbon capture. However, the most critical component of the SCLP-OXY-CC unit can be related to the solar field and tower, together with the need for new system additions including solid handling units, reactors for reduction and oxidation, an additional power generating station among others. This would incur considerable capital investments for the necessary retrofit. The cost of the solar fields was obtained from a recent study by Falter et al [38], which was then modified to the necessary scale.

Table 6 Capital Cost Breakdown of the proposed *SCLP-OXY-CC* unit

| Plant Component | Values (million) | % Contribution |
|---|---|---|
| Primary Gas turbine, generator and auxiliaries | $1.33 | 0.88% |
| HRSG, ducting and stack | $2.47 | 1.64% |
| Steam turbine, generator and auxiliaries, | $5.74 | 3.82% |
| Cooling Water System and Balance of Plant | $6.35 | 4.22% |
| $CO_2$ Recycle Compressor | $3.16 | 2.10% |
| Pump for $H_2O$ | $0.02 | 0.01% |
| $CO_2$ Compressor for CL Unit | $0.97 | 0.65% |
| Syngas Compressor ($H_2$) | $28.54 | 19.00% |
| ASU (Complete CAPEX) | $0.15 | 0.10% |

| | | |
|---|---|---|
| Other Heat Exchangers | $0.04 | 0.03% |
| Solar Reactor | $7.08 | 4.71% |
| Reflectors | $20.60 | 13.71% |
| Receiver Cost | $7.08 | 4.71% |
| Solar Tower | $0.83 | 0.55% |
| Total Equipment Costs (TEC) | $84.21 | 56.05% |
| Cost of metal oxide loading | $0.01 | 0.01% |
| Total Intsallation Costs | $34.00 | 22.63% |
| Total Direct Plant Cost (TDPC) | $118.37 | 78.78% |
| Indirect Costs | $16.57 | 11.03% |
| Engineering Procurement and Construction Costs (EPC) | $134.94 | 89.81% |
| Owner's Costs | $1.66 | 1.10% |
| Contingencies | $13.49 | 8.98% |
| ASU (Complete CAPEX as an add-on unit) | $0.15 | 0.10% |
| Total Project Costs (TPC) | $150.25 | 100.00% |

Table 6 represents the cost breakdown of the proposed SCLP-OXY-CC unit. The ASU was assumed as an add-on unit, with a CAPEX of $150,000. However, the major contributor to the overall CAPEX is from the Solar Field and its associated components. The reflectors form the costliest of all the equipment, accounting for over 13.7% of the total plant CAPEX and 29.2% of the TEC. The combined solar field, including the reflectors, receiver, tower and reactor account for almost 36% of the overall equipment costs. However, the costliest equipment is the hydrogen compressor, which accounts for 19% alone of the TPC. This is due to its high cost of equipment working under pure hydrogen environments [39]. The net project CAPEX was obtained at around $150 million, which amounts to around 12,136 $/kW, a cost, much higher than the present day specific cost of electricity producing units, and especially for traditional solar tower based concentrated solar power producing plants [40,41].

In addition, the operational expenses were calculated based on the assumptions mentioned in the earlier section. A capacity factor of 25% was assumed for a CSP without storage based on literature [41]. The net fixed OPEX was obtained as $7.02 million, while the variable cost was calculated as 1.42 $/MWh of gross power generation. Hence a net annual operating cost of $15.05 million was calculated to run the proposed 12.8 MW SCLP-OXY-CC unit.

### 5.3 Levelized cost of electricity (LCOE)

LCOE calculations were hence developed based on equation (22) with assumptions listed in Table 1 to perform a comparative evaluation of the system economic performance. As mentioned, no carbon tax was assumed. Correspondingly an LCOE of 1,100 $/MWh was obtained. The cost attained is well over current technologies and hence incentives or carbon credits are crucial to make such a system economically competitive. In addition, economics of scale can be understood to play a severe role, a higher capacity would tremendously benefit the specific CAPEX of the proposed unit. However, it is to be mentioned, that if $CO_2$ would be utilized only and no water for splitting purposes, the cost of the components can be decreased further, that can result in significant economic benefits of the proposed system.

## 6 Conclusions

A comprehensive solar thermochemical looping $CO_2/H_2O$ splitting model was developed in ASPEN Plus to simulate the chemical looping syngas fuel generation from water and carbon dioxide splitting in a dual moving bed reactor with redox cycling through metal oxides. An extensive FORTRAN subroutine was developed and hooked into ASPEN Plus to appropriately model the complexities of the reaction kinetics and the two-phase flow within the reactors. The entire set-up was evaluated considering industrial scale applications and hence generation of 100 mol/s of syngas fuel. An isothermal reduction reactor and an

adiabatic oxidation reactor model was developed and evaluated. A maximum reduction non-stoichiometry of 0.198 was obtained in the reduction reactor at 1600$^{o}$C and $10^{-7}$ bar pressure. The residence time was around 1.5 minutes, an increase in residence time will not yield any further benefit due to a faster backward reaction rate of recombination of the released oxygen in the reduction reactor. The volume of the oxidation reactor to achieve an over 90% conversion of the reduced metal oxide was 8 times higher to the volume of the reduction reactor. The impact of the variation of the gas inlet temperature was found to be minimal, while an increase in the metal oxide inlet temperature would significantly increase the solid conversion and selectivity of the generated syngas fuel. A faster water splitting kinetics would result in not only a higher solid conversion and selectivity, but also in a higher product outlet temperature due to higher exothermicity. Indeed, a relatively substantial increase in the yields from the oxidation reactor with 25% water in the gas mixture is noticed than while working with pure $CO_2$. Nevertheless, similar selectivity from co-splitting of $CO_2$ and $H_2O$ would allow generating the $H_2$/CO ratio similar to the input $H_2O/CO_2$ ratio, a major benefit of the moving bed reactor system. A large temperature variation long the length of the adiabatic oxidation reactor is also noticed, which would thus require further reaction design optimization of the moving bed oxidation reactor for $CO_2$ and/or $H_2O$ splitting. This gives the motivation to further investigate the reactor model as a chemical looping syngas production unit as an add-on unit to the power plant and investigate the efficiency of the system.

The CL unit model was then integrated to a proposed power plant layout to be implemented as an add-on unit to an existing Oxyfuel power plant with CCS. Retrofitting a 100 MW Oxyfuel NGCC was thus evaluated with multiple sensitivity studies varying different operating parameters and composition of the gas to the oxidation reactor of the CL unit. Utilizing 20% of the $CO_2$ generated for CCS, a maximum of 12.85 MW of electricity can be generated, which can be improved subject to system optimization. A maximum solar to

electricity efficiency of 25.4% was obtained while working with $CO_2$ only and operating the reduction reactor at 1600$^oC$ and $10^{-7}$ bar vacuum pressure. The oxidation reactor was operated at 2 bar pressure. Considerable variation in the output of the system is noticed with the variation of the reduction temperature, which would often limit the steady operation of the system to only a few hours of the day without storage. Economic analysis has been carried out and found that the major contributor to CAPEX is solar field related components and equipment accounting to nearly 36% of the cumulative equipment costs. Apart from that hydrogen compressor cost is 19% of total project cost. The specific overnight capital cost is 12136 $/kW which is very high compare to traditionally produced by solar tower technology. The levelized cost of electricity is evaluated to be 1100 $/MWh. The cost of the of separation of oxygen for oxyfuel combustion could be reduced by replacing with more advanced technologies such as ion transport membranes which could also increase the efficiency of the system as well as reduce the total equipment cost. Apart from this, CAPEX could be reduced if only $CO_2$ splitting is carried out through thermochemical looping as the cost of hydrogen compressor is huge.

**References:**


[1] D.Y.C. Leung, G. Caramanna, M.M. Maroto-Valer, An overview of current status of carbon dioxide capture and storage technologies, Renew. Sustain. Energy Rev. 39 (2014) 426–443. doi:10.1016/j.rser.2014.07.093.

[2] Y.A. Daza, R.A. Kent, M.M. Yung, J.N. Kuhn, Carbon dioxide conversion by reverse water-gas shift chemical looping on perovskite-type oxides, Ind. Eng. Chem. Res. 53 (2014) 5828–5837. doi:10.1021/ie5002185.

[3] J. Kim, C.A. Henao, T.A. Johnson, D.E. Dedrick, J.E. Miller, E.B. Stechel, C.T. Maravelias, Methanol production from CO2 using solar-thermal energy: process development and techno-economic analysis, Energy Environ. Sci. 4 (2011) 3122. doi:10.1039/c1ee01311d.

[4] S. Abanades, H.I. Villafan-Vidales, CO2 and H2O conversion to solar fuels via two-step solar thermochemical looping using iron oxide redox pair, Chem. Eng. J. 175 (2011) 368–375. doi:10.1016/j.cej.2011.09.124.

[5] S. Abanades, G. Flamant, Thermochemical hydrogen production from a two-step solar-driven water-splitting cycle based on cerium oxides, Sol. Energy. 80 (2006)

1611–1623. doi:10.1016/j.solener.2005.12.005.

[6] P. Furler, J.R. Scheffe, A. Steinfeld, Syngas production by simultaneous splitting of H2O and CO 2 via ceria redox reactions in a high-temperature solar reactor, Energy Environ. Sci. 5 (2012) 6098–6103. doi:10.1039/C1EE02620H.

[7] M.M. Hossain, H.I. de Lasa, Chemical-looping combustion (CLC) for inherent CO2 separations-a review, Chem. Eng. Sci. 63 (2008) 4433–4451. doi:10.1016/j.ces.2008.05.028.

[8] D. Yadav, R. Banerjee, A review of solar thermochemical processes, Renew. Sustain. Energy Rev. 54 (2016) 497–532. doi:10.1016/j.rser.2015.10.026.

[9] V.M. Wheeler, J. Zapata, P. Kreider, W. Lipinski, Effect of non-stoichiometry on optical, radiative, and thermal characteristics of ceria undergoing reduction, Opt. Express. 26 (2018) 1238–1243. doi:10.1364/oe-26-10-A360.

[10] A. Steinfeld, Solar thermochemical production of hydrogen - A review, Sol. Energy. 78 (2005) 603–615. doi:10.1016/j.solener.2003.12.012.

[11] B.D. Ehrhart, C.L. Muhich, I. Al-Shankiti, A.W. Weimer, System efficiency for two-step metal oxide solar thermochemical hydrogen production – Part 1: Thermodynamic model and impact of oxidation kinetics, Int. J. Hydrogen Energy. 41 (2016) 19881–19893. doi:10.1016/j.ijhydene.2016.07.109.

[12] B. Bulfin, A.J. Lowe, K.A. Keogh, B.E. Murphy, O. Lübben, S.A. Krasnikov, I. V. Shvets, Analytical Model of CeO 2 Oxidation and Reduction, J. Phys. Chem. C. 117 (2013) 24129–24137. doi:10.1021/jp406578z.

[13] D. Arifin, Study of redox reactions to split water and carbon dioxide, University of Colorado, 2013. http://scholar.colorado.edu/chbe_gradetds/54.

[14] R.W. Breault, E.R. Monazam, J.T. Carpenter, Analysis of hematite re-oxidation in the chemical looping process, Appl. Energy. 157 (2015) 174–182. doi:10.1016/j.apenergy.2015.08.015.

[15] C. Zhou, K. Shah, H. Song, J. Zanganeh, E. Doroodchi, B. Moghtaderi, Integration Options and Economic Analysis of an Integrated Chemical Looping Air Separation Process for Oxy-fuel Combustion, Energy & Fuels. 30 (2016) 1741–1755. doi:10.1021/acs.energyfuels.5b02209.

[16] S. Mukherjee, P. Kumar, A. Yang, P. Fennell, Energy and exergy analysis of chemical looping combustion technology and comparison with pre-combustion and oxy-fuel combustion technologies for CO2 capture, J. Environ. Chem. Eng. 3 (2015) 2104–2114. doi:10.1016/j.jece.2015.07.018.

[17] H. Kong, Y. Hao, H. Wang, A solar thermochemical fuel production system integrated with fossil fuel heat recuperation, Appl. Therm. Eng. 108 (2016) 958–966. doi:10.1016/j.applthermaleng.2016.03.170.

[18] H. Kong, Y. Hao, H. Jin, Isothermal versus two-temperature solar thermochemical fuel synthesis: A comparative study, Appl. Energy. 228 (2018) 301–308. doi:10.1016/j.apenergy.2018.05.099.

[19] K. Jana, A. Ray, M.M. Majoumerd, M. Assadi, S. De, Polygeneration as a future

sustainable energy solution – A comprehensive review, Appl. Energy. 202 (2017) 88–111. doi:10.1016/j.apenergy.2017.05.129.

[20] R. Stanger, T. Wall, R. Spörl, M. Paneru, S. Grathwohl, M. Weidmann, G. Scheffknecht, D. McDonald, K. Myöhänen, J. Ritvanen, Oxyfuel combustion for CO2 capture in power plants, Int. J. Greenh. Gas Control. 40 (2015) 55–125. doi:http://dx.doi.org/10.1016/j.ijggc.2015.06.010.

[21] J. Mletzko, S. Ehlers, A. Kather, Comparison of natural gas combined cycle power plants with post combustion and oxyfuel technology at different CO2 capture rates, Energy Procedia. 86 (2016) 2–11. doi:10.1016/j.egypro.2016.01.001.

[22] S. Nazir, O. Bolland, S. Amini, Analysis of Combined Cycle Power Plants with Chemical Looping Reforming of Natural Gas and Pre-Combustion CO2 Capture, Energies. 11 (2018) 147. doi:10.3390/en11010147.

[23] C.L. Muhich, B.D. Ehrhart, I. Al-Shankiti, B.J. Ward, C.B. Musgrave, A.W. Weimer, A review and perspective of efficient hydrogen generation via solar thermal water splitting, Wiley Interdiscip. Rev. Energy Environ. 5 (2016) 261–287. doi:10.1002/wene.174.

[24] Mitsubishi Heavy Industries, Gas Turbines, (n.d.). https://www.mhi.com/products/energy/gas_turbine.html (accessed May 23, 2018).

[25] Wärtsilä, Gas Turbine for Power Generation: Introduction, (2018). https://www.wartsila.com/energy/learning-center/technical-comparisons/gas-turbine-for-power-generation-introduction (accessed May 29, 2018).

[26] J. Fan, L. Zhu, P. Jiang, L. Li, H. Liu, Comparative exergy analysis of chemical looping combustion thermally coupled and conventional steam methane reforming for hydrogen production, J. Clean. Prod. 131 (2016) 247–258. doi:10.1016/j.jclepro.2016.05.040.

[27] A. Farooqui, A. Bose, D. Ferrero, J. Llorca, M. Santarelli, Techno-economic and exergetic assessment of an oxy-fuel power plant fueled by syngas produced by chemical looping CO2 and H2O dissociation, J. CO2 Util. 27 (2018) 500–517. doi:10.1016/j.jcou.2018.09.001.

[28] A. Mutuberria, J. Pascual, M. V. Guisado, F. Mallor, Comparison of Heliostat Field Layout Design Methodologies and Impact on Power Plant Efficiency, Energy Procedia. 69 (2015) 1360–1370. doi:10.1016/j.egypro.2015.03.135.

[29] B. Ehrhart, D. Gill, Evaluation of annual efficiencies of high temperature central receiver concentrated solar power plants with thermal energy storage, Energy Procedia. 49 (2013) 752–761. doi:10.1016/j.egypro.2014.03.081.

[30] G.P. Hammond, Engineering sustainability : thermodynamics , energy systems , and the environment, 639 (2004) 613–639. doi:10.1002/er.988.

[31] A. Bejan, Thermal Design and Optimzation, John Wiley, New York, 1996.

[32] S. Sievers, T. Seifert, M. Franzen, G. Schembecker, C. Bramsiepe, Fixed capital investment estimation for modular production plants, Chem. Eng. Sci. 158 (2017) 395–410. doi:10.1016/j.ces.2016.09.029.

[33] C. Cormos, Integrated assessment of IGCC power generation technology with carbon capture and storage ( CCS ), Energy. 42 (2012) 434–445. doi:10.1016/j.energy.2012.03.025.

[34] Politecnico di Milano - CAESER Project, European best practice guidelines for assessment of CO2 capture technologies, 2011.

[35] Politecnico di Milano – Alstom UK (CAESAR project), European best practice guidelines for assessment of CO2 capture technologies., (2011).

[36] IEA, Executive Summary - Projected Costs of Generating Electricity, 2015. https://www.oecd-nea.org/ndd/pubs/2015/7057-proj-costs-electricity-2015.pdf.

[37] Eurostat, Natural gas price statistics, EU-28, (2016) 1–12. doi:http://ec.europa.eu/eurostat/statistics-explained/index.php/Natural_gas_price_statistics.

[38] C. Falter, V. Batteiger, A. Sizmann, Climate Impact and Economic Feasibility of Solar Thermochemical Jet Fuel Production, Environ. Sci. Technol. 50 (2016) 470–477. doi:10.1021/acs.est.5b03515.

[39] J. Apt, A. Newcomer, L.B. Lave, S. Douglas, L.M. Dunn, An Engineering-Economic Analysis of Syngas Storage, U.S. Dep. Energy's Natl. Energy Technol. Lab. (2008) 143.

[40] Capital Cost Estimates for Utility Scale Electricity Generating Plants, 2016. https://www.eia.gov/analysis/studies/powerplants/capitalcost/pdf/capcost_assumption.pdf.

[41] IRENA, Renewable Energy Technologies Cost Analysis Series: Concentrating Solar Power, Compr. Renew. Energy. 3 (2012) 595–636. doi:10.1016/B978-0-08-087872-0.00319-X.